Materials and Structures (2015) 48:629–641
DOI 10.1617/s11527-014-0461-x

ORIGINAL ARTICLE

Effect of slag chemistry on the hydration of alkali-activated blast-furnace slag

Ricarda Tänzer · Anja Buchwald · Dietmar Stephan

Received: 22 April 2014 / Accepted: 23 October 2014 / Published online: 20 November 2014

Abstract This paper presents results of detailed investigations about the alkaline activation of ground granulated blast furnace slags whose chemical composition were modified. Sodium hydroxide and potassium silicates were used as alkaline activators. The influence of the CaO/SiO_2 ratio, the Al_2O_3 and TiO_2 content of the slag composition on the hydration reaction was analyzed utilizing isothermal heat flow calorimetry, compressive strength development of binder samples, ^{29}Si MAS NMR spectroscopy and molybdate method. It could be shown that the TiO_2 content of the slag has only minor influence on the hydraulic reactivity and compressive strength of the alkaline activated binders.The variation of the Al_2O_3 content of the slag leads to different results. A rise in Al_2O_3 content enhanced the strength if activating with NaOH but resulted in a lower strength if activating with potassium silicate. The results of the ^{29}Si MAS NMR spectroscopy verify the decrease in the reaction degree with increase of Al_2O_3 content. This is associated with the rise of the chain length of the C-(A)-S–H phases by incorporation of Al–O tetrahedrons resulting in a lower Si/Al-ratio. A decrease in the C/S-ratio yielded to a lower heat evolution, whereas the reaction was delayed if activated with potassium silicate with higher silicate content. The increase of the C/S-ratio caused in less condensed slag glass and therefore an enhancement of the reaction degree with a simultaneous decrease of silicate chain length, as seen by ^{29}Si NMR. These outcomes fit well with the results measured by the molybdate method.

Keywords Ground granulated blast-furnace slag · Alkali silicates · Alkali activation · ^{29}Si NMR · Molybdate method

R. Tänzer (✉) · D. Stephan
Building Materials and Construction Chemistry, Technische Universität Berlin, Gustav-Meyer-Allee 25, 13355 Berlin, Germany
e-mail: ricarda.taenzer@tu-berlin.de

A. Buchwald
ASCEM B.V, Schaarweg 4, 6991 GV Rheden, The Netherlands

1 Introduction and background

Granulated blast furnace slag, a by-product of the raw iron production, is almost exclusively used as a main ingredient of standard cements in Germany so far. A key aspect of slag research is therefore the identification of assessment criteria for the reactivity of ground granulated blast furnace slag (GGBFS). The positive effect of some oxides (CaO, MgO, K_2O, Na_2O) or the adverse effect of a high content of SiO_2, TiO_2 or MnO in the GGBFS on its reactivity are known [1]. However these indicators only allow a very rough estimate of the reactivity of blast furnace slag as a cement component [2, 3]. Additionally various empirical indicators (Table 1, [4–9]) are used for the correlation between

chemical composition and technical properties [4, 10]. These indicators does not predict reliable the properties of the resulting cements. Key parameters of the production process itself such as temperature in the furnace, viscosity of the liquid slag and conditions for granulation may also play an important role [11, 12]. For that reason the compressive strength of mortars made from the cements containing these GGBFS is used as a safe evaluation criterion. The influence of different major and minor components of the GGBFS on the strength development was investigated frequently. Especially the influence of the Al_2O_3 content on the strength development because of an increased basicity was documented rather early [2] resulting in a positive influence on the early age strength, which may have a negative effect on the strength at later ages. The correlation between the chemical–mineralogical composition of the slag and the properties of the resulting binder have to be asked again with the upcoming interest in utilizing GGBFS for the production of alkali activated materials. If GGBFS is activated with alkali hydroxides, carbonates or silicates the correlations known for the activation with Portland cement might be not further valid or even more complex. Sakulich et al. [13] investigated the influence of adding Al_2O_3 to slags activated with NaOH/water glass solutions. The increase in compressive strength after 7 and 28 days was observed if adding low amounts of Al_2O_3, whereas a further addition of Al_2O_3 caused a delay of the hydration and did not enhance the mechanical properties. Ben Haha et al. [14] investigated slags with different Al_2O_3 contents activated with NaOH and sodium silicate solutions. It was found using isothermal calorimetry that an increased Al_2O_3 content of the slag slows down the rate of hydration. A high Al_2O_3 content resulted in a clear delay of the main reaction peak if activating with silicate solution, but accelerated the main reaction peak if activating with NaOH. In fact a lower strength at early ages was reached with higher Al_2O_3 content compared to the original slag but no significant differences at later times.

There are only few studies about the influence of MgO in slags. Ben Haha et al. [15] could show that an increasing MgO content of the slag from 8 to 13 wt% accelerated the reaction and resulted in higher compressive strengths. How much the reaction will be accelerated depended on the type of activator. A faster reaction and a higher strength was achieved using NaOH as activator instead of sodium silicate. The differences between slags containing little or much MgO were more distinctive if activating with sodium silicate, although comparable degrees of slag reaction were detected. Bernal et al. [16] showed that a low content of MgO content leads to a faster reaction (in contrast to the results published by Ben Haha), whereas the overall extent of reaction was reduced. Both Bernal and Ben Haha [15, 16] verified that a lower MgO content favors the incorporation of Al–O tetrahedrons into the C–S–H chains.

Table 1 Selection of different empirical indicators for correlation of chemical composition and technical characteristics of GGBFS [4]

Empirical indicators	Suggestion/source (year)
$p_1 = \frac{CaO}{SiO_2} > 1$	"Basic" basicity (1885) [5]
$p_2 = \frac{CaO+MgO}{SiO_2} > 1$	DIN EN 197-1 (2011) [6]
$CaO + MgO + SiO_2 > 2/3$	DIN EN 15167-1 (2006) [7]
$p_3 = \frac{CaO+MgO}{SiO_2+Al_2O_3} \geq 1$	German standard for "slag Portland cement" (1909) [8]
$F = \frac{CaO+1/2S^{2-}+1/2MgO+Al_2O_3}{SiO_2+MnO} > 1.5$	F-value by Keil [9]

Studies on cements containing blast furnace slag have demonstrated that the TiO_2 content of GGBFS has a substantial influence on the reaction behavior and that an increased TiO_2 content >1 wt% has a negative effect on the strength development [4]. According to Wolter et al. and Wang et al. [17, 18] TiO_2 in the melt is present as Ti^{4+} and Ti^{3+} and can replace Si^{4+} acting as a network former in the glass network. This results in a densification of the glass structure and the increase of particle density as well as corrosion resistance. Subsequent the higher corrosion resistance leads to a worse dissolution of the glass network.

The production conditions of the slag have a significant influence and were different in diverse investigations which impede a clear correlation between the chemical–mineralogical composition of the GGBFS and its technical behavior towards individual activators could be derived [19]. The way out could be the use of synthetic slag. It is possible to pursue the influence of different parameters (basicity, Al_2O_3 content etc.) of the blast furnace slag without having a superposition of different chemical and other influences, as it is inevitably when using different industrially produced granulated slags. This way is

Table 2 Chemical composition of the GGBFSs utilized

GGBFS	CaO wt%	SiO_2	Al_2O_3	MgO	TiO_2	S_{total}	C/S –
S1	42.5	34.8	**11.4**	8.3	**0.5**	0.8	**1.22**
S2	41.6	34.4	12.0	8.2	**1.9**	0.6	1.21
S3	37.7	31.0	**21.6**	7.3	0.4	0.8	1.22
S4	45.4	31.9	13.3	7.8	0.4	0.4	**1.42**
S5	35.2	41.1	13.7	7.8	0.6	0.3	**0.86**

Bold numbers are the criteria which are compared

chosen for the investigations described. The basis was a conventional GGBFS which was modified by adding several oxides, re-molten and granulated again and milled under identical laboratory conditions. The focus was set on the influence of the CaO/SiO_2 ratio, the Al_2O_3 and TiO_2 content.

2 Materials and methods

2.1 Ground granulated blast furnace slag (GGBFS) and alkaline activators

The original base material of the studies was an industrial GGBFS. This slag was modified with pure oxides to reach the desired composition and re-molten in a graphite crucible under nitrogen atmosphere at temperatures between 1,550 and 1,650 °C. Subsequently it was granulated in a laboratory wet granulation system. This procedure was chosen to guarantee absolute identical production conditions for all slags investigated to pursue the influence of certain chemical constituents on the reactivity of the GGBFS. In this paper, however, the influence of the basicity (C/S-ratio),[1] the TiO_2 content and the Al_2O_3 content of the slag will be discussed. Table 2 summarizes the chemical characteristics of the GGBFSs used. The glass content was determined by light microscopy. Therefore the crystalline and glassy components of 1,000 slag grains (fraction 40–63 μm) were counted [20]. The glass content was determined between 98 and 100 wt%. The slags were ground in a ball mill for the further use as binder material. The particle size distributions of the grinded GGBFSs were comparable to each other with d_{50} values of 11–12 μm and Blaine fineness between 4,100 and 4,300 cm^2/g. Only GGBFS S2 was slightly finer with a d_{50} value of 9 μm and a Blaine fineness of approximately 4,800 cm^2/g.

Sodium hydroxide (NaOH) and two potassium silicate solutions with molar water glass modules (SiO_2/M_2O) of 1 and 2 were used as alkaline activators (Table 3). Furthermore a water/slag-ratio of 0.35 was defined for all alkali-activated binders to allow a comparability between them, because of the different solid contents of the alkaline solutions used. Pure binder paste samples without any aggregates were prepared and used in all investigations.

2.2 Experimental investigation

At first the binder reaction of the alkali-activated GGBFSs were followed by isothermal heat flow calorimetry (TAMair, Thermometric) at 20 °C. Sample specimen measuring $2 \times 2 \times 2$ cm^3 were prepared for mechanical testing of the hardened binders. The samples were kept in moulds at 20 °C for one day, then demoulded and stored afterwards at 20 °C and 100 % RH until the date of testing the compressive strength. In order to characterize the reaction products the hydration was stopped by means of vacuum drying at day 1, 7, 28 and 180 after preparation. The dried samples were ground to a fineness <63 μm.

^{29}Si nuclear magnetic resonance spectroscopy (MAS NMR) is a method for quantification of the silicate phases which deemed to be the most suitable method in these amorphous systems. Solid state NMR experiments were performed with a Bruker Avance 300 spectrometer (magnetic field strength 7.0455 T, resonance frequency of ^{29}Si is 59.63 Hz). To measure the ^{29}Si MAS NMR spectra, the samples were packed in 7 mm zirconia rotors and spun at 5 kHz at an angle of 54°44′. The chemical shifts were recorded relative to external tetramethylsilane (TMS). The single pulse technique was applied with a pulse width of 4 μs. According to the high paramagnetic portion of the samples, a short repetition time of 5 s was chosen and a typical number of scans were 40,000. Thirty Hertz line broadening was applied to all spectra prior to deconvolution. The quantitative analysis that means the deconvolution of the signal patterns of the spectra was done with the software PeakFit of Scientific Solutions.

A second method for characterization of silicate species is the so called "molybdate method". Silicate

[1] Cement nomenclature: C = CaO, S = SiO_2.

Table 3 Chemical composition of the used activators and binders

Solution						Binder	
	$n_{alkali}/m_{solution}$	Mass-content				Mass-ratio	
	mol/kg	Na_2O wt%	K_2O	SiO_2	Total solid	m_{Na2O}/m_{GGBFS} %	m_{K2O}/m_{GGBFS}
NaOH	2.0	6.2	–	–	6.2	2.4	–
K-WG-1	2.0	–	9.4	6.0	15.4	–	3.6
K-WG-2	2.0	–	9.4	12.0	21.4	–	3.6

species react in sulphuric acid (pH value of 1–2) with ammonium heptamolybdate solution [$(NH)_4Mo_7O_{24}$-$4H_2O$] to yellow-colored β-silico-molybdic acid complex ($H_4SiMo_{12}O_{40}$) [21–23]. The reaction progress can be monitored by UV–Vis spectrometry at a wavelength of 400 nm. The temperature was always set to 25 °C. The hydrolysis obeys the rate law of first order, and therefore it is possible to conclude from the rate constant to the degree of condensation of the silicate contained in the sample [23]. However the evaluation of the results is not clearly in the case of alumosilicates, because of the dissolution of the sample in acid in what the Al–O–Si bonds will be broken. Therefore only the degree of condensation of the (remaining) silicates can be measured [24]. The longer the reaction takes, the higher was the condensation of silicate in the binder, which is indicated by the rate constant k. It is possible to deduce the amount of SiO_2 units in the reaction products from the determined rate constant by comparing with values of known silicate species [23, 25–28]. Furthermore, the degree of condensation of the silicate contained in the sample can be calculated using the maximum extinction. This value is based on the SiO_2 content of the binder, which is calculated from the composition of the raw materials (slag + activator) and the loss on ignition of the binder. Inasmuch it could have been come to minor changes due to carbonation during preparation of the binder (e.g. reaction, grinding), solely the tendency of the "molybdate active SiO_2" can be considered.

3 Results and discussions

3.1 Isothermal calorimetry

Figure 1 shows the isothermal heat flow calorimetry of different GGBFSs activated with sodium hydroxide and potassium silicate solutions.

Wolter et al. and Wang et al. [17, 18] reported that TiO_2 can replace Si^{4+} in the glass network resulting in a densification of the glass structure and a higher corrosion resistance. If this higher corrosion resistance is influencing the activation with sodium hydroxide and potassium silicate this should be measurable with heat flow calorimetry. Figure 1a depicts that S2 (high TiO_2 content) shows a lower heat flow which is 1.5 h delayed compared to S1 if activated with K-WG-1. However the cumulated heat after 72 h was nearly the same (Table 4). In case of using NaOH as activator both heat flow curves look similar but the cumulated heat of the reaction of S2 is 12 % higher than that of S1. Presumably this might be related to the higher fineness of S2 (4,800 cm^2/g instead of approx. 4,200 cm^2/g).

The modification of the Al_2O_3 content led not to a systematic correlation to the hydraulic reactivity of the slag. The highest heat flow maximum occurred of activating GGBFS S3 (high Al_2O_3 content of 21.6 wt%) with NaOH (Fig. 1b) which is in agreement with the results of Ben Haha et al. [14]. The cumulated heat of S3 was higher compared to the binder with S1 (low Al_2O_3 content). The activation of both GGBFSs with K-WG-1 show contrary results. The intensity of the heat flow peak of S3 was lower but at an earlier time than of that of S1. The observed results of the main hydration peak are similar to that of the initial peak found by Ben Haha. He measured an initial peak in the first minutes and a second main peak which showed a long dormant period of more than 60 h. Such a second, delayed peak could not be observed. It has to be mentioned that the samples were mixed outside the calorimeter. Therefore it is not possible to follow the first minutes of the reaction.

The influence of the C/S-ratio was studied on the slags S1, S4 and S5. The C/S-ratio ranges from 0.86 for S5 over 1.22 for S1 to 1.42 for S4. If the basicity of the slag (C/S-ratio) rises, the content of CaO increases

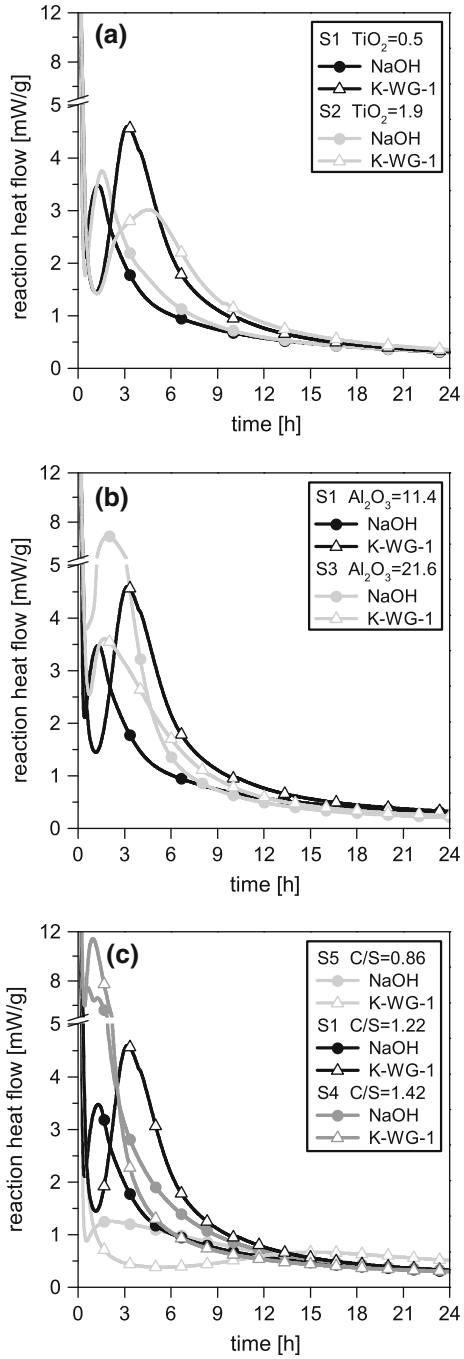

Fig. 1 Isothermal heat flow calorimetry of different GGBFSs with sodium hydroxide and potassium silicate as activator, comparison of different **a** TiO_2 contents in wt%, **b** Al_2O_3 contents in wt% **c** C/S-ratios

with a simultaneous decrease of SiO_2 which leads to an expansion of the glass network and facilitate splitting of existing Si–O-bonds. This usually results in a better dissolution/reactivity of the slag and a faster strength development. The question arises if this increasing reactivity has an impact if different alkaline activators are used. Figure 1c shows the heat flow of the binders activated with NaOH and K-WG-1. For NaOH, the enhanced reactivity of S4 compared to S1 and S5 is characterized by an increased intensity in the heat flow as well as a significantly higher heat release (Table 4). After 72 h the heat of hydration of the samples S1 and S5 is 28 % respectively 37 % lower than that of S4. If the same samples were activated with silicate (K-WG-1) a distinct time shift is seen in addition to the steplike heat flow maxima. The binder with S4 again showed the highest heat release. The heat release of the binder with S5 is with 32 % less compared to the binder with S4 and thus almost the same as for the activation with NaOH. But the difference of the heat release of the binder with S1 compared to S4 is only 8 % less (within 72 h). The reason for this is supposedly that the activator NaOH is stronger in the beginning. More hydroxide ions could dissolve the slag glass and the mean reaction as characterized by the heat flow was measured during the first 6 h. The hydroxide concentration of the K-WG-1 silicate solution was lower and dissolved the slag glass slower but the incorporation of additional SiO_2 in the reaction products resulted in a larger amount of heat released within the first 72 h.

3.2 Compressive strength

Figure 2 shows the compressive strength development of different GGBFSs activated with sodium hydroxide and potassium silicate as activators.

The influence of the TiO_2 contents on the compressive strength (Fig. 2a) is much more significant than on the heat flow calorimetry. If activating with NaOH the 28 days strength of the binder with S2 (high TiO_2 content of 1.9 wt%) is 74 % higher than that of the binder with S1 (low TiO_2 content of 0.5 wt%) while it is only 8 % higher if activating with K-WG-1. But with K-WG-1 the deviation in compressive strength is in some cases significantly higher than that for the binder with NaOH. Even if it can be supposed that a part of the strength results from the slightly higher fineness of the GGBFS S2, it can be assumed that no major losses in the hydraulic reactivity of S2 compared with S1 can be observed in alkali-activated binders. The strength reduction as known from

Table 4 Cumulative heat released after 3, 6, 12, 24 and 72 h (J/g)

GGBFS	TiO_2	Al_2O_3	C/S	Activator	Time (h)				
	wt%		–		3	6	12	24	72
S1	0.5	11.4	1.22	NaOH	43.4	58.2	74.6	92.4	121.1
S2	1.9	12.0	1.21		47.5	66.5	84.7	102.6	135.4
S3	0.4	21.6	1.22		71.8	102.1	119.1	132.4	153.1
S4	0.4	13.3	1.42		70.0	93.7	115.9	135.5	167.7
S5	0.6	13.7	0.86		26.4	38.6	56.6	75.5	105.2
S1	0.5	11.4	1.22	K-WG-1	46.7	85.0	111.4	132.0	162.2
S2	1.9	12.0	1.21		40.3	71.3	102.9	126.0	160.0
S3	0.4	21.6	1.22		52.8	78.6	100.2	115.7	139.2
S4	0.4	13.3	1.42		94.5	111.9	127.4	144.0	176.7
S5	0.6	13.7	0.86		26.7	31.0	41.2	67.6	119.4

cements containing GGBFS with higher TiO_2 contents and Portland cement clinker [4, 18] might be related to the other type of activation by $Ca(OH)_2$, which is formed during the hydration of C_3S and C_2S. There is still no explanation for the different mechanisms. But therefore the alkaline activation is of special interest for GGBFSs with high TiO_2, as these cannot be sufficiently activated with Portland cement clinker.

The compressive strength of the binder with S3 (high Al_2O_3 content of 21.6 wt%) activated with NaOH was significantly increased compared to those of S1 (Fig. 2b). After 1 day the compressive strength of the binder with S3 is 3 times higher and after 28 days and 180 days they are still almost twice as high as the strength values of the binder with S1. This confirms the experiences with blast furnace slag cements [29]. A completely different performance emerged if activating S1 and S3 with potassium silicate (K-WG-1). In this case the binder with S1 obtained higher strength over the entire duration of the measurement than that of the binder with S3. In addition the compressive strength of the binder with S3 activated with K-WG-2 is pictured. The doubling of the SiO_2 content in the activator resulted in a significant rise in the compressive strength development especially after 28 and 180 days.

The early strengths after 1 day (Fig. 2c) were influenced by the C/S-ratio. The binder with S4 (C/S = 1.42) activated with NaOH reached the highest strength and the binder with S5 (C/S = 0.86) activated with K-WG-1 reached the lowest strength after 1 day reaction. Interestingly, this negative effect of low basicity is compensated over time regarding the binder with K-WG-1. After 180 days the strength of the binder with S5 (C/S = 0.86) exceeded even that of the other binder with higher C/S (S1 and S4). The reasoning is that the initial phase of the reaction is influenced by dissolving the glass, in which a high pH value of the activator has a positive effect. The subsequent course of the reaction goes together with a densification of the structure, which is achieved by precipitated and incorporated SiO_2.

3.3 Nuclear magnetic resonance spectroscopy

The ^{29}Si NMR spectrum in Fig. 3 shows the modification of the glass network of GGBFS. Table 5 lists the values of the ^{29}Si chemical shift of the different GGBFS glass peaks.

According to Wolter et al. [17] even low TiO_2 contents lead to changes in the glass structure. In the blast furnace slag glass Ti is simultaneously present in the oxidations states Ti^{4+} and Ti^{3+}. According to the network hypothesis of Zachariasen [30, 31] Ti^{4+} can replace Si^{4+} in the network as a network former, while Ti^{3+} preferably represents the Ca^{2+} instead. But in octahedral coordination it tightens the network in contrast to Ca^{2+} [17]. Various studies on titanosilicates showed that the Ti is present in these compounds in octahedral coordination (TiO_6). These TiO_6 octahedra are linked to corner-sharing SiO_4 tetrahedra through bridging oxygen atoms. Similar to aluminosilicates a systematic downfield shift in the Si-NMR spectra can be seen with increasing titanium next-nearest neighbors. Labouriau et al. have measured the following shifts for different SiO_4 environments: 0Si,4Ti = −78.5 ppm; 1 Si,3Ti = −82.0 ppm; 2Si,2Ti = −90.6 ppm and 3Si,1Ti = −94.2 ppm

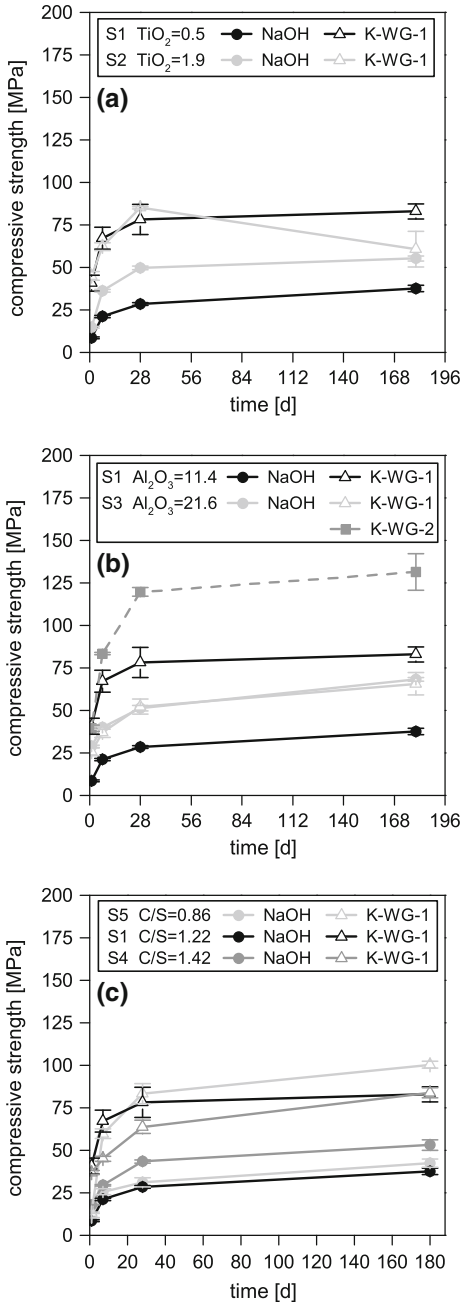

Fig. 2 Compressive strength development of different GGBFSs with sodium hydroxide and potassium silicate as activator, comparison of different **a** TiO_2 contents in wt%, **b** Al_2O_3 contents in wt% **c** C/S-ratios

[32]. Balmer et al. reported that the effect on the chemical shift depends on the charge of the bond between Si and Ti. A Si bond to tetrahedral Ti has a formal charge of 0, and therefore no effect is expected [33]. The peak position of S2 with the significantly

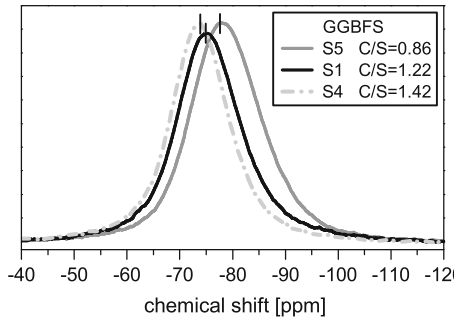

Fig. 3 ^{29}Si NMR–chemical shifts of GGBFS with different C/S-ratios

Table 5 ^{29}Si MAS NMR spectroscopy of origin GGBFS glass and alkaline activated binders-peak positions and curve parameter used for deconvolution

GGBFS/ reaction product	Chemical shift (ppm)	Half width (ppm)	Gauss/ Lorentz ratio
S1	−75.4	13.9	0.40
S2	−75.2	14.0	0.46
S3	−76.3	14.2	0.44
S4	−73.8	12.7	0.43
S5	−78.2	15.5	0.44
Q_1 (−78 ± 2 ppm)	−78.4	4.3	0.0001
Q_2(1Al) (−82 ± 2 ppm)	−81.2	4.3	0.0001
Q_2 (−85 ± 2 ppm)	−84.2	4.3	0.0001
Q_{poly} (precipitated silicate)	−88.3	8.6	0.0001

increased TiO_2 content was found almost identical to the position of S1, the GGBFS with normal TiO_2 content. Due to the minimal change in the peak positions either the Ti occurs in tetrahedral coordination or the concentration of TiO_2 in the GGBFS is too low to detect a clear shift. On the other hand, a content of nearly 2 wt% TiO_2 is relatively high for industrial practice already and lead to significantly altered reaction behavior of the GGBFS [4].

Al_2O_3 in the glass can function as a network modifier and as a network former [34]. The shift of a SiO_4 group depend on the degree of SiO_4 polymerization (Q_n) and the number of Si or Al atoms in the second coordination sphere of the central silicon. In general, each substitution of a Si atom by an Al atom causes a down field shift of about 5 ppm [35]. In Table 5 it can be seen that an increase of the Al_2O_3

content (S1 and S3) resulted in a slight shift of the peak maxima to higher field in the ^{29}Si NMR spectra, which is attributed to the function of Al_2O_3 as a network former.

Figure 3 shows the ^{29}Si NMR spectra of the GGBFSs with varied basicity(C/S-ratio). A rising C/S-ratio means that the content of CaO increases with a simultaneous decrease of SiO_2 which will result in a less condensed glass network. Conversely, the glass network is higher condensed at a low C/S-ratio, which can be seen in the ^{29}Si NMR spectrum by a clear upfield shift. With increasing polymerization of Q_n building units a characteristic upfield shift is observed in solid silicates from about −65 ppm for Q_0 in monosilicates up to about −110 ppm for Q_4 groups in fully polymerized silica. One condensation step ($Q_0 \rightarrow Q_1 \rightarrow Q_2 \rightarrow Q_3 \rightarrow Q_4$) is correlated to a peak shift of approximately 10 ppm. [35] Starting from S1 which has a C/S-ratio of 1.22, the peak of S5 (C/S-ratio 0.86) is shifted upfield and the peak of S4 (C/S-ratio 1.42) is shifted downfield, as expected.

The quantitative determination of the reaction products of alkali-activated GGBFS was done after 28 days of hydration. In some cases the measurements showed overlapping signals, for which reason three binders were re-examined after 180 days of hydration.

The reaction products of alkali-activated slags can quantitatively be determined by a peak deconvolution. From the known peak parameters of the blast furnace slag (−74 ± 2 ppm respectively Table 5) and C-(A)-S–H phases (Q_1: −78 ± 2 ppm, Q_2(1Al): −82 ± 2 ppm, Q_2: −85 ± 2 ppm) a theoretical curve was calculated and approximated to the measured data by only changing the amount of the single signals in such way that a minimum deviation was achieved. This gives information about the proportions of the individual signals for the different chemical environments of the silicon atom. First, the pure GGBFS were adjusted by setting a glass peak. Afterwards the 180 days old binder with S1 activated with NaOH was selected to define the peak parameter of the C-(A)-S–H phases Q_1, Q_2(1Al) and Q_2. These parameters (Table 5) were considered for further evaluation as constant. It is assumed that the C-(A)-S–H phases of the same system will have the same peak position and shape. A similar approach was described in [36, 37].

The GGBFS activated with potassium silicates had an additional signal showed up as a broad shoulder around −90 ppm. There are approaches which correlated these signals with aluminosilicate compounds (Q_4(3Al) and Q_4(2Al)), such as in alkali-activated mixtures of blast furnace slag and metakaolin [38]. Another possible explanation could be that pure silicate gel is precipitated. If silicate is mixed with blast furnace slag, it can lead to a withdrawal of colloid or constitution water resulting in a condensation of colloidal silica oligomers due to the large surface of GGBFS particles that has to be wetted [39, 40]. Therefore silicate bridges between the slag particles might be formed, which condensated during solidification and formed solid gel structures [40]. Brough et al. [41] as well observed a signal which is substantially at −90 ppm. They assigned this peak to cross-linked calcium or aluminum substituted silicate species, which they summarized as Q_{poly} for all polymerized silicate species in general. For this reason, a 180 day old binder S3 activated with K-WG-2 was used to identify the signal of the "precipitated silicate" (Q_{poly}). Figure 4 shows the deconvoluted ^{29}Si NMR spectra of the 28 and 180 days old binder of slag S1 activated with NaOH as exemplary results of the deconvolution.

From the deconvolution results, the degree of reaction (DR) of GGBFS, the average chain length (mean chain length-MCL) and the Si/Al-ratio of the C-(A)-S–H phases are calculated [35, 38, 42, 43]. The formulas are quoted elsewhere [38]. The calculation results are listed in Table 6.

By comparing the results of the 28 and 180 days old samples an increase in the degree of reaction can be observed in all three samples with increasing age, which is significantly higher in the binder with S1 than in the binder with S3. The Si/Al-ratio increases slightly with increasing age of the binder activated with NaOH, while it remains constant for the sample activated with potassium silicate. The binder with S3 shows a slightly lower Si/Al-ratio in comparison to the binder with S1 (both activated with NaOH). This means that more Al_2O_3 was incorporated into the chains of the C-(A)-S–H phases. If silicate is used as activator, extra Si is introduced into the system, which on the one hand is available as "precipitated silicate" and on the other hand can be integrated into the C-(A)-S–H phases. Thus, the Al content is reduced in the C-(A)-S–H phases and their Si/Al-ratio increases. The longest chain lengths were calculated for S3 activated with NaOH.

The NMR results of Table 6 can also be sorted by GGBFS characteristics. Slag with high C/S-ratio has a

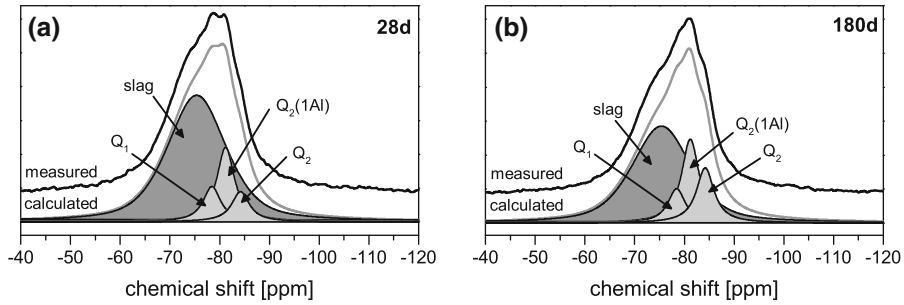

Fig. 4 Deconvoluted ^{29}Si MAS NMR spectra of alkali-activated slag paste of S1 and NaOH at the age of **a** 28 days and **b** 180 days

Table 6 Calculation results (mol% Si) of deconvolution of the signal patterns of the spectra and calculated results of DR, MCL and Si/Al of the activated binder

GGBFS	Activator	Sample age	Q_{poly} (precipitated silicate)	C-(A)-S–H phases			Glass peak of GGBFS	C-(A)-S–H phases		DR
				Q_2	$Q_2(1Al)$	Q_1		MCL	Si/Al	
		(days)	−89 ppm	−85 ppm	−82 ppm	−79 ppm	∼ −75 ppm see Table 5			
			(mol% Si)					–	–	%
S1	NaOH	180	0.0	12.8	19.4	8.0	59.8	12.5	4.1	40.2
S3			0.0	8.7	17.7	4.2	69.4	18.6	3.5	30.6
S3	K-WG-2		13.4	12.4	11.3	9.0	53.9	8.6	5.8	32.7
S1	NaOH	28	0.0	6.3	15.5	7.4	70.8	10.0	3.8	29.2
S2			0.0	7.0	15.6	8.5	68.9	9.2	4.0	31.1
S3			0.0	5.0	17.7	3.8	73.5	18.5	3.0	26.5
S4			0.0	8.7	15.3	12.9	63.1	6.9	4.8	36.9
S5			0.0	7.1	7.7	3.4	81.8	13.0	4.7	18.2
S3	K-WG-1		4.5	9.7	11.2	3.8	70.8	16.1	4.4	24.7
S5			12.9	13.4	7.3	5.1	61.3	11.6	7.1	25.8
S3	K-WG-2		13.4	11.7	9.8	6.9	58.3	9.7	5.8	28.4

depolymerized glass network, which can be split of quickly by an alkaline activator. This leads to a rapid formation of many small nuclei and a rapid growth of the reaction products, which are therefore of shorter length. The binders with S5, S1 and S4 clearly show an increase in the degree of reaction with increasing C/S-ratio, with a simultaneous decrease of the chain length. This is reflected in significantly different strength developments (see Fig. 2). Comparing the samples with different TiO_2 contents (S1, S2), only very small differences in chain length, degree of reaction and Si/Al-ratio can be observed. That reflects no clear influence of the TiO_2 content on the reactivity of GGBFS within alkaline activated systems. Maybe the concentrations of TiO_2 in the slags are too low, or the alkaline activation is not negatively influenced by TiO_2. The increase of Al_2O_3 content caused a decrease in the degree of reaction, which could be attributed to the function of Al_2O_3 as a network former (slight upfield shift of the glass peak in Table 5). It has further be noticed that the average chain length of 18 was very high. This can partly be explained by the incorporation of Al into the C-(A)-S–H phases, which resulted in a lower Si/Al-ratio. It is noteworthy that the rise in Al_2O_3 content resulted in a significant increase in particular the early strength (Fig. 2).

Finally, it is possible to classify the results in Table 6 of S3 (GGBFS with high Al_2O_3 content) and S5 (GGBFS with low C/S ratio) according to different activators. If the effect of the activators NaOH, K-WG-1 and K-WG-2 is compared for the reaction of S3 it can be noticed, that the SiO_2 content of the activator increases with increasing water glass module from 0 (for hydroxide) to 2 and therefore the SiO_2

Table 7 Calculated results (% SiO_2 molybdate active, rate constant k) of the activated binder

GGBFS	Al_2O_3 (wt%)	C/S(-)	Activator	Age (days)	% SiO_2 molybdate active	Rate constant k (min^{-1})	Time interval for calculation of k (min)
S5	13.7	0.86	NaOH	28	79.7	0.33	0.5–7
						0.07	7–31
S1	11.4	1.22			98.7	0.57	0.5–7
S4	13.3	1.42			103.9	0.55	0.5–7
S5	13.7	0.86	K-WG-1	28	80.6	0.28	0.5–7
						0.12	7–25
S1	11.4	1.22			97.0	0.50	0.5–7
S4	13.3	1.42			108.0	0.45	0.5–7
S1	11.4	1.22	K-WG-1	1	96.1	0.64	0.5–7
				7	99.1	0.47	0.5–7
				28	97.0	0.50	0.5–7
				180	106.7	0.58	0.5–3
						0.27	3–10
S3	21.6	1.22	K-WG-2	1	84.8	0.45	0.5–7
				7	86.3	0.40	0.5–7
						0.20	7–12
				28	86.4	0.37	0.5–7
						0.10	7–19
				180	108.6	0.40	0.5–7
						0.04	7–29

content in the overall system. The Si/Al-ratio reflects this very well. With increasing SiO_2 content in the overall system more SiO_2 was incorporated into the C-(A)-S–H phases than Al_2O_3. This reduced the bridging effect of the Al_2O_3 and the average chain length was reduced. Furthermore, the proportion of "precipitated silicate" raised with increasing SiO_2 content of the activator. S5 is less reactive due to its low C/S-ratio, but also for this slag could be confirmed, that the increasing SiO_2 content of the activators led to a rise of the Si/Al-ratio and consequently to a decrease in the chain length.

3.4 Molybdate method

The degree of linkage of the SiO_2 in the sample can be inferred from the reaction kinetic of the silicate to the yellow colored β-silico-molybdic acid complex. In the case of alumosilicates only the degree of condensation of the (remaining) silicates can be measured [24], because of the dissolution of the sample in acid in what the Al–O–Si bonds will be broken.

The pure slag samples reacted completely within 3 min to β-silico-molybdic acid. The calculated rate constants of 1.2−1.5 min^{-1} indicate a mixture of monomeric and dimeric silicate species.

The results of the measured binders include information of the slag glass and the formed reaction products. A clear separation and quantification is difficult. Therefore Table 7 lists the rate constants and in addition the time intervals, which were used for calculation. For some samples two rate constants could be calculated by two straight portions of the curve.

Figure 5a, b shows the formation rates of β-silico-molybdic acid for alkali activated binders with different C/S-ratios of the slag activated with NaOH and K-WG-1. Comparing these results in the upper part of Table 7, it is found that the amount of molybdate active SiO_2 decreases from about 100 to 80 % with decreasing C/S-ratio for both activators NaOH and K-WG-1 for 28 day old samples. This means that a part of the silicate species in the binder is so long that it cannot be measured with the molybdate method, which explains the lower proportion of molybdate active SiO_2. The rate constant

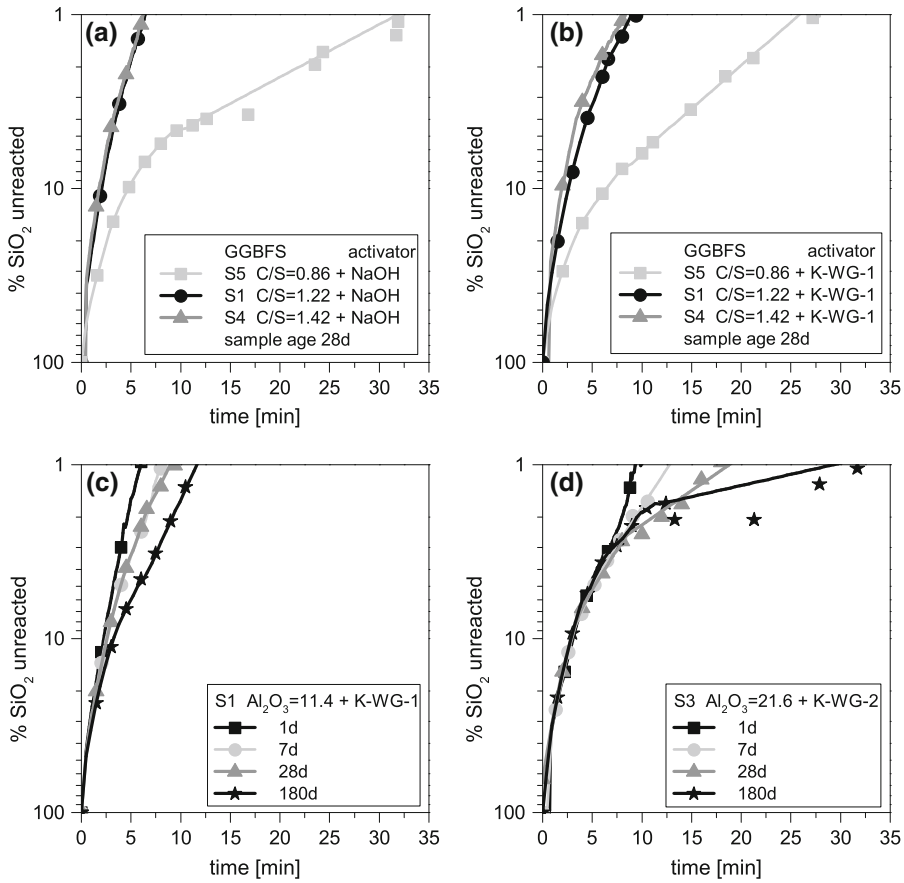

Fig. 5 Formation rates of β-silico-molybdic acid for alkali activated binders with different CaO/SiO_2 ratios of the slag activated with **a** NaOH and **b** K-WG-1 as well as binders with different Al_2O_3 contents of the slag activated with **c** K-WG-1 and **d** K-WG-2 at different age

decreases as well, which indicates oligomer silicate species. The rate constants of 0.33 and 0.28 (S5 with C/S = 0.86) as found for the 28 day old samples activated with NaOH and K-WG-1 respectively, indicate a SiO_2 unit length of about 8–10, while the rate constants between 0.45 and 0.57 (S1 and S4 with C/S = 1.22 and 1.42 respectively) point out to a length of 6–8 SiO_2 units. The sample S5 (C/S = 0.86) activated with NaOH contains in addition a small amount of polysilicates (rate constant of 0.07) and in the binder with S5 activated with K-WG-1 some of the silicate species are longer than 10 SiO_2 units (rate constant of 0.12).

Figure 5c, d show binder samples, which were measured after different sample age. With increasing sample age, the increase in conversion curves declines and more time is needed for the reaction of the SiO_2 to the yellow β-silico-molybdic acid complex. This is also semi-quantitative illustrated by the decreasing rate constants (the bottom half of Table 7). With increasing sample age a transformation of the silicate species took place from smaller oligomers to longer chains with more SiO_2 units. In the case of S1 and K-WG-1, the rate constants from 0.47 to 0.64 indicate chain lengths of about 6-8 SiO_2 units for 1–28 day old samples. After 180 days some of the silicate species were about 8–10 SiO_2 units long (rate constant of 0.27). The binder which consists of S3 and K-WG-2 formed longer reaction products of 8–10 SiO_2 units (rate constants from 0.37 to 0.45). This was probably due to the increased SiO_2 content of the activator. Already after 7 days a small amount of silicates is higher polymerized (about 10 SiO_2 units, rate constant of 0.20) than the other silicates. With further sample age the chain length grew to silicate species longer 10 SiO_2 units (rate constant of 0.10 after 28 days) and polysilicates (rate constant of 0.04 after 180 days).

4 Summary

An increase in TiO_2 content leads to a slight acceleration of the hydration in the case of K-WG-1. But a

significant impact on the hydration observed by calorimetry was not visible. The influence of the TiO_2 contents on the compressive strength was much more significant. An increase of TiO_2 content causes higher strength especially by activation with NaOH which is at least partly due to the higher fineness of the slag with the highest TiO_2 content. But nevertheless it can be assumed that with alkaline activation no major losses in the hydraulic reactivity of slags with high TiO_2 content will be observed. The results in ^{29}Si NMR show only very small differences in the degree of reaction, chain length and Si/Al-ratio of the reaction products C-(A)-S–H phases.

Changing the Al_2O_3 content of the slag did not lead to a systematic change in the hydraulic reactivity. It strongly depends on the used activator. The same was observed by measuring the compressive strength. A rise in Al_2O_3 content enhances the strength when activated with NaOH but reduces it when activated with K-WG-1. The results of ^{29}Si NMR depict a decrease in the degree of reaction with increase of Al_2O_3 content in the slag glass. Simultaneously the chain length rises by incorporation of Al in the C-(A)-S–H phases, which reveals in a lower Si/Al-ratio.

The impact of the CaO/SiO_2 ratio on the reactivity depends on the activator. A decrease in the C/S-ratio yields in case of K-WG-1 to a delay of hydration and in case of NaOH and K-WG-1 in a lower heat evolution. The C/S-ratio influences the early strengths after 1 day in the same way. A low C/S-ratio results in a low compressive strength and a high C/S-ratio implicate a high compressive strength. But regarding the binder with K-WG-1 this behavior is changing. The late strength of the slag with the lowest C/S-ratio exceeds the other binders. This is due to a densification of the structure by precipitated SiO_2. Regarding the results of ^{29}Si NMR it could be measured that an increase of the C/S-ratio causes in less condensed slag glass and therefore show an enhancement in the degree of reaction, with a simultaneous decrease of chain length. This decrease in chain length could also be detected with the molybdate method for NaOH as well as for K-WG-1 as activator. Furthermore the calculated chain lengths of 7–13 (^{29}Si NMR) for the binders with NaOH fit well with the calculated chain lengths of 6–10 measured by the molybdate method.

Acknowledgments The authors thank Dr. A. Ehrenberg (FEhS) and Dr. J. Krakehl (Woellner) for the supply of slag and waterglass, Dr. H. Hilbig (cbm, TU Munich) for the NMR measurements and A. Dobbertin for support in the lab. The investigations presented here, were funded by the AiF on behalf of the German Federal Ministry for Economics and Technology in the project "Alkali activated ground granulated blast-furnace slags for concrete application under aggressive conditions (IGF project 15800 BG)" and the German Federal Ministry of Education and Research in the project "Chemically Bonded Ceramics by Nanotechnological Improvements of Structure (03X0067G)".

References

1. Forschungsgemeinschaft-Eisenhüttenschlacken (2000) Iron and steel slags-properties and utilisation-Reports from 1974–2000, Duisburg
2. Smolczyk HG (1978) Zum Einfluß der Chemie des Hüttensands auf die Festigkeiten von Hochofenzementen. ZKG Int 31(6):294–296
3. Schröder F (1961) Über die hydraulischen Eigenschaften von Hüttensanden und ihre Beurteilungsmethoden. Tonindustrie-Zeitung 85(2/3):39–44
4. Ehrenberg A (2006) Hüttensand-Ein leistungsfähiger Baustoff mit Tradition und Zukunft-Teil 2. Beton-Informationen (5):67–95
5. Tetmajer L (1886) Der Schlackenzement. Stahl und Eisen 6(7):473–483
6. DIN EN 197-1 (2011) Zement-Teil 1 Zusammensetzung, Anforderungen und Konformitätskriterien von Normalzement
7. DIN EN 15167-1 (2005) Hüttensand zur Verwendung in Beton, Mörtel und Einpressmörtel - Teil 1. Definitionen, Anforderungen und Konformitätskriterien
8. Deutsche Normen für einheitliche Lieferung und Prüfung von Eisenportland-Zement (1909)
9. Keil F (1963) Hochofenschlacke. Stahleisen-Bücher Band 7. Verlag Stahleisen mbH, Düsseldorf
10. Ehrenberg A, Wilhelm D, Kühn A et al (2008) Granulated blastfurnace slag-reaction potential and production of optimized cements, Part 2. Cem Int 6(3):82–92
11. Mußgnug G (1938) Die hydraulischen Eigenschaften der Hochofenschlacke. Mitteilungen aus den Forschungsanstalten des GHH-Konzerns 6(7):153–180
12. Dölbor F (1963) Einfluß der Abkühlungsbedingungen und der chemischen Zusammensetzung auf die hydraulischen Eigenschaften von Hämatitschlacken. Doctoral Thesis
13. Sakulich AR, Anderson E, Schauer CL et al (2010) Influence of Si: Al ratio on the microstructural and mechanical properties of a fine-limestone aggregate alkali-activated slag concrete. Mater Struct 43(7):1025–1035
14. Ben Haha M, Lothenbach B, Le Saout G et al (2012) Influence of slag chemistry on the hydration of alkali-activated blast-furnace slag-Part II: effect of Al_2O_3. Cem Concr Res 42(1):74–83

15. Ben Haha M, Lothenbach B, Le Saout G et al (2011) Influence of slag chemistry on the hydration of alkali-activated blast-furnace slag-Part I. Eff MgO Cem Concr Res 41(9):955–963
16. Bernal SA, San Nicolas R, Myers RJ et al (2014) MgO content of slag controls phase evolution and structural changes induced by accelerated carbonation in alkali-activated binders. Cem Concr Res 57:33–43
17. Wolter A, Frischat GH, Olbrich E (2003) Investigation of granulated blast furnace slag (GBFS) reactivity by SNMS. In: 11th International Congress on the Chemistry of Cement
18. Wang PZ, Rudert V, Lang E et al (2002) Influence of the TiO_2 content on the reactivity of granulated blastfurnace slags. Cem Int 1(1):120–128
19. Stephan D, Tänzer R, Braun T et al (2010) Alkali activation–an alternative to binders that contain clinker; Part 1/2. Cem Int 8(1/2):72–85/74–81
20. Drissen P (1994) Glasgehaltsbestimmung von Hüttensand. ZKG Int 47(11):658–661
21. Stade H (1978) Zur Bildungskinetik der ß-Dodekamolybdatokieselsäure. I. Die Umsetzung von monokieselsäure mit Molybdänsäure. Z Anorg Allg Chem 441(1):29–38
22. Stade H (1978) Zur Bildungskinetik der β-Dodekamolybdatokieselsäure. II. Die Umsetzung von kondensierten Kieselsäuren mit Molybdänsäure. Z Anorg Allg Chem 446(1):5–16
23. Thilo E, Wieker W, Stade H (1965) Chemische Untersuchungen von Silicaten, XXXI. Über Beziehungen zwischen dem Polymerisationsgrad silicatischer Anionen und ihrem Reaktionsvermögen mit Molybdänsäure. Z Anorg Allg Chem 340(5–6):261–276
24. Hoebbel D, Garzó G, Ujszászi K et al (1982) Herstellung und Anionenkonstitution von kristallinen Tetramethylammonium-alumosilicaten und -alumosilicatlösungen. Z Anorg Allg Chem 484(1):7–21
25. Hoebbel D, Ebert R, Wieker W et al (1988) Über die Anwendung der Farbstoffadsorptionsmethode zur Charakterisierung von Natriumsilicat-(Wasserglas-) lösungen. Z Anorg Allg Chem 558(1):171–188
26. Hoebbel D, Wieker W (1971) Die Konstitution des Tetramethylammoniumsilicats der Zusammensetzung 1,0 N(CH3) 4OH 1,0 SiO2 · 8,0–8,3 H2O. Z Anorg Allg Chem 384(1): 43–52
27. O'Connor TL (1961) The reaction rates of polysilicic acids with molybdic acid. J Phys Chem 65(1):1–5
28. Hübert C. et al. (received 2013) Collection of rate constants k of different silicate species, B TU Cottbus-Senftenberg
29. Wang PZ, Trettin R, Rudert V et al (2004) Influence of Al_2O_3 content on hydraulic reactivity of granulated blastfurnace slag, and the interaction between Al_2O_3 and CaO. Adv Cem Res 16(1):1–7
30. Zachariasen WH (1932) The atomic arrangement in glass. J Am Chem Soc 54(10):3841–3851
31. Zachariasen WH (1933) Die Struktur der Gläser. Glastechnische Berichte 11
32. Labouriau A, Higley TJ, Earl WL (1998) Chemical shift prediction in the ^{29}Si MAS NMR of titanosilicates. J Phys Chem B 102(16):2897–2904
33. Balmer ML, Bunker BC, Wang LQ et al (1997) Solid-state ^{29}Si MAS NMR study of titanosilicates. J Phys Chem B 101(45):9170–9179
34. Shi C, Krivenko PV, Roy D (2006) Alkali-activated cements and concrete. Taylor and Francis, New York
35. Engelhardt G, Michel D (1987) High Resolution solid state NMR of silicates and zeolithes. Wiley, Chichester
36. Schilling PJ, Butler LG, Roy A et al (1994) ^{29}Si and ^{27}Al MAS-NMR of NaOH-activated blast-furnace slag. J Am Ceram Soc 77(9):2363–2368
37. Schneider J, Cincotto MA, Panepucci H (2001) ^{29}Si and ^{27}Al high-resolution NMR characterization of calcium silicate hydrate phases in activated blast-furnace slag pastes. Cem Concr Res 31(7):993–1001
38. Buchwald A, Hilbig H, Kaps C (2007) Alkali-activated metakaolin-slag blends-performance and structure in dependence of their composition. J Mater Sci 42(9):3024–3032
39. Goberis S, Antonovich V (2004) Influence of sodium silicate amount on the setting time and EXO temperature of a complex binder consisting of high-aluminate cement, liquid glass and metallurgical slag. Cem Concr Res 34(10):1939–1941
40. Zellmann HD, Ch K (2006) Chemically modified waterglass binders for acid-resistant mortars. J Am Ceram Soc 89(4):1369–1372
41. Brough AR, Holloway M, Sykes J et al (2000) Sodium silicate-based alkali-activated slag mortars Part II. The retarding effect of additions of sodium chloride or malic acid. Cem Concr Res 30(9):1375–1379
42. Hilbig H, Buchwald A (2006) The effect of activator concentration on reaction degree and structure formation of alkali-activated ground granulated blast furnace slag. J Mater Sci 41(19):6488–6491
43. Andersen MD, Jakobsen HJ, Skibsted J (2004) Characterization of white Portland cement hydration and the C-S-H structure in the presence of sodium aluminate by ^{27}Al and ^{29}Si MAS NMR spectroscopy. Cem Concr Res 34:857–868